Supplementary Information To

Electronics and optoelectronics of lateral heterostructures within monolayer indium monochalcogenide

Hao Jin[1], Jianwei Li[1], Bin Wang[1], Yunjin Yu[1], Langhui Wan[1], Fuming Xu[1], Ying Dai[2], Yadong Wei[1],* and Hong Guo[1]

[1]*College of Physics and Technology, Shenzhen University, Shenzhen 518060, People's Republic of China.*

[2]*School of Physics, State Key Laboratory of Crystal Materials, Jinan, 250100, People's Republic of China.*

Band structures of InX monolayers

The single-layer InX (X=S, Se, Te) consists of four sublayers, which stack in the sequence of X-In-In-X. Unlike TMDs materials, bulk InX materials have direct bandgaps, whereas their monolayers are indirect band-gap semiconductors. The calculated band structures of single-layer InX obtained by PBE and HSE06 functionals are shown in **Figure S1**. It can be seen in all cases that, VBM of InX materials locates between the Γ and M points, while the CBM occurs at either M point for InTe or Γ point for InS and InSe monolayers. As the chalcogen species changes from S to Te, the band gaps decrease, which can be attributed to the decrease in ionicity [1, 2]. Note that PBE and HSE06 functionals give similar trend of band structures despite the band gaps. So in this paper, the results are mainly discussed at the PBE level.

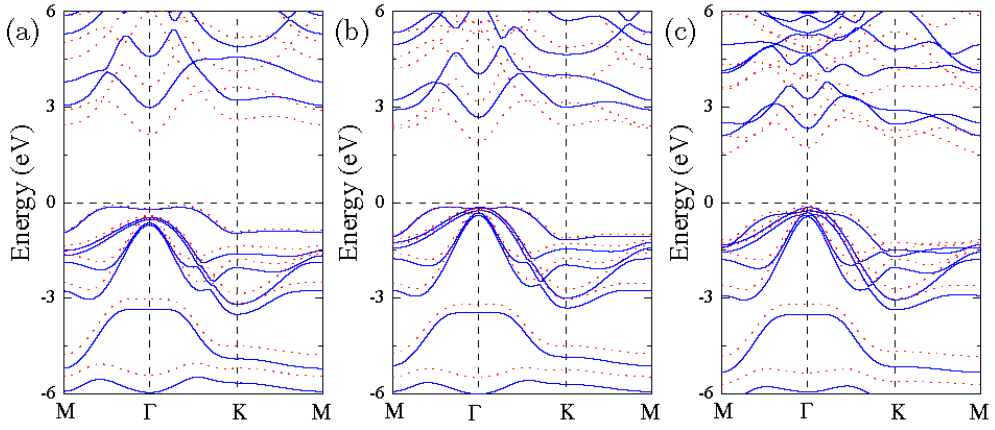

Figure S1. The calculated band structures of InX (X=S, Se, Te) by PBE (red dash lines) and HSE06 (blue solid lines) functional, respectively. The Fermi level is set to zero.

DOS for InSe-InTe heterostructure

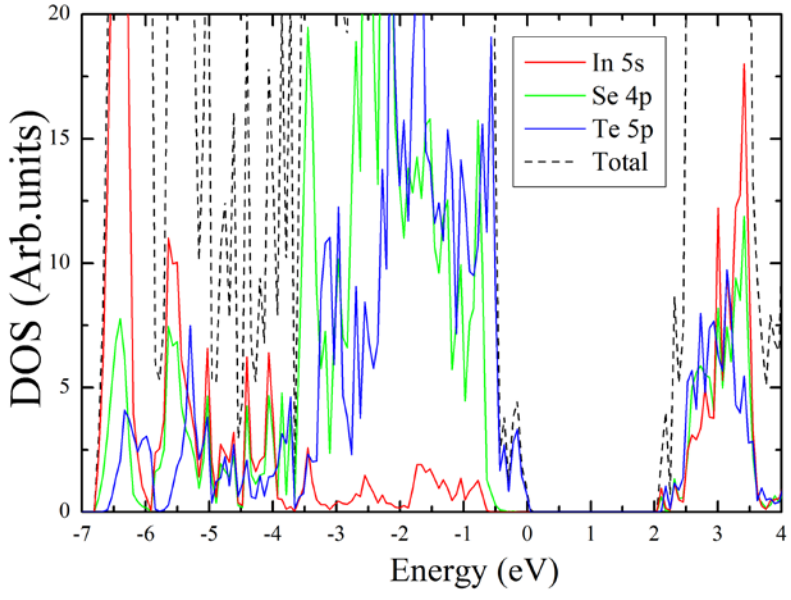

Figure S2. Calculated projected density of states (PDOS) for InSe-InTe lateral heterointerface at its optimized structure via HSE06 functional. The In 5*s* and Se 4*p* states at InSe side are indicated by the red and green solid lines, while the Te 5*p* states at InTe side are represent by the blue solid lines. The Fermi level is set to be zero.

Strain engineering

The strain-induced bandgap engineering has recently been demonstrated to be a powerful technique [3]. To check the influence of the strain on the stability and electronic structures of lateral heterinterfaces, we study the interface energy as a function of the lattice constants. In this work, the interface energy

(γ_{hi}) is calculated as:[4]

$$\gamma_{hi} = \frac{1}{2S_0}(E_{X-Y} - E_X - E_Y) \qquad \text{(S1)}$$

where S_0 is the area of the lateral heterointerface. E_X and E_Y are the total energies of the supercell for different InX (X=S, Se, Te) monolayers, respectively. $E_{X\text{-}Y}$ is the total energy of the supercell containing the lateral interfaces. The factor 2 comes from two heterointerfaces included in the supercell. The results are shown in **Figure S3.** The optimized lattice constant for InS-InSe heterostructure is 3.89 Å, which is very close to the average value of the lattice constants of InS and InSe monolayers. Similar result is also obtained for InSe-InTe heterostructure, and its optimized lattice constant is 4.11 Å.

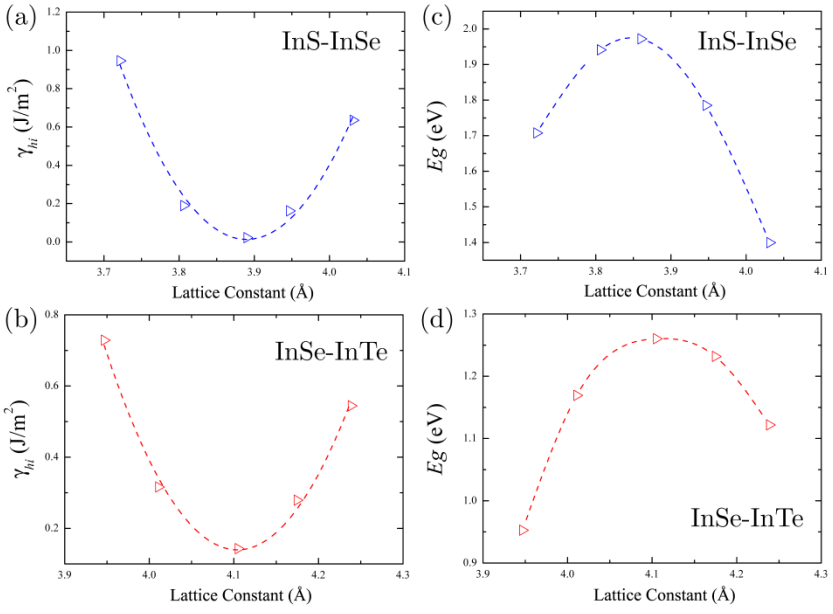

Figure S3. The calculated heterointerface energies as a function of lattice constant for (a) InS-InSe and (b) InSe-InTe in-plane heterojunctions. The band gaps as a function of lattice constant for (c) InS-InSe and (d) InSe-InTe in-plane heterojunctions.

Figure S3 shows that in both cases, the lateral heterointerfaces have the maximum values of the band gaps at their optimized structures. When the lattice constants deviate from their optimized structures, the band gap will decrease simultaneously by about 30% and 25% for InS-InSe and InSe-InTe lateral heterostructures under about 4% tensile or compressive strains, respectively.

Photocurrent of MoS_2 monolayer

To check the accuracy of our computations, we calculate the photocurrent of MoS_2 monolayer based on the same methodology used in the manuscript. The results are shown in **Fig. S4**. The calculated photocurrent reaches the maximum values at 459 nm. According to **Eq. 11** in the manuscript, the maximum photoresponse (R_{ph}) is calculated with the value of 17.3 mA/W, which is in good agreement with the experimental measurement, i.e. 16 mA/W (see **Table 2** of the manuscript), indicating the method employed in this work is reliable.

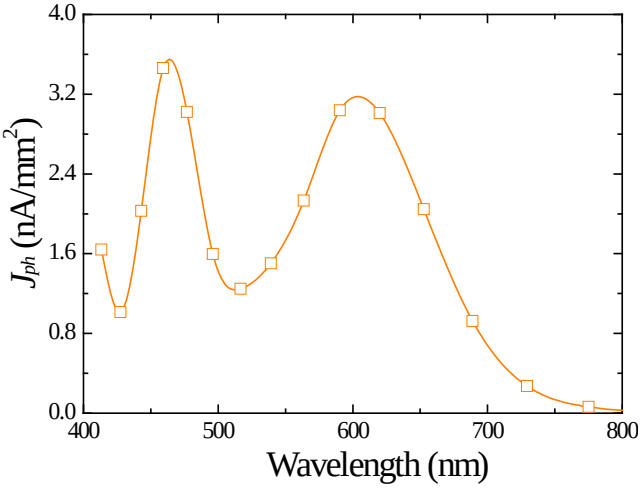

Fig. S4. Calculated photocurrents of MoS_2 monolayer as a function of wavelength. The incident light power density is 0.2 μW/mm^2.

References

1. W. A. Harrison, *Electronic structure and the properties of solids:the physics of the chemical bond*, Freeman, New York, 1989.
2. H. L. Zhuang and R. G. Hennig, *Chemistry of Materials*, 2013, **25**, 3232-3238.
3. X. Li, Y. Dai, M. Li, W. Wei and B. Huang, *Journal of Materials Chemistry A*, 2015, **3**, 24055-24063.
4. H. Jin, I. Elfimov and M. Militzer, *Journal of Applied Physics*, 2014, **115**, 152-156.